

Different Active-Site Loop Orientation in Serine Hydrolases versus Acyltransferases

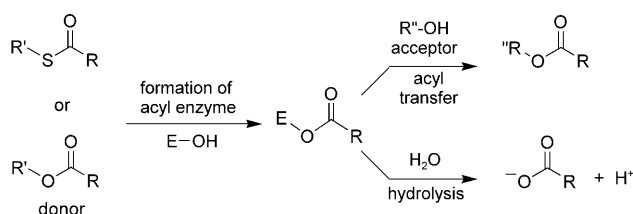
Yun Jiang,^[a] Krista L. Morley,^[b] Joseph D. Schrag,^{*,[c]} and Romas J. Kazlauskas^{*,[a]}

Acyl transfer is a key reaction in biosynthesis, including synthesis of antibiotics and polyesters. Although researchers have long recognized the similar protein fold and catalytic machinery in acyltransferases and hydrolases, the molecular basis for the different reactivity has been a long-standing mystery. By comparison of X-ray structures, we identified a different oxyanion-loop orientation in the active site. In esterases/lipases a carbonyl oxygen points toward the active site, whereas in acyltransferases a NH of the main-chain amide points toward the active site. Amino acid sequence comparisons alone cannot identify such a difference in the main-chain orientation. To

identify how this difference might change the reaction mechanism, we solved the X-ray crystal structure of *Pseudomonas fluorescens* esterase containing a sulfonate transition-state analogue bound to the active-site serine. This structure mimics the transition state for the attack of water on the acyl-enzyme and shows a bridging water molecule between the carbonyl oxygen mentioned above and the sulfonyl oxygen that mimics the attacking water. A possible mechanistic role for this bridging water molecule is to position and activate the attacking water molecule in hydrolases, but to deactivate the attacking water molecule in acyl transferases.

Introduction

Acyltransferases (EC number 2.3) catalyze the transfer of an acyl group from a donor, usually an ester or thioester, to an acceptor, usually an alcohol or amine, thereby forming esters or amides (Scheme 1). Some acyltransferases are called thioester-



Scheme 1. Acyltransferases catalyze the transfer of an acyl group from a donor (ester or thioester) to an acceptor (alcohol in this example). Both hydrolases and acyltransferase form an acyl-enzyme intermediate, but hydrolases transfer the acyl group to water, whereas acyltransferases transfer it to an acceptor.

ases for their homology to fatty acyl thioesterases. In fatty acid biosynthesis, these thioesterases catalyze hydrolysis, but the thioesterase domains in polyketide biosynthesis and nonribosomal peptide biosynthesis can catalyze either hydrolysis or acyl transfer. The acyl transfer reaction is similar to the hydrolysis reaction catalyzed by carboxyesterases and lipases (EC number 3.1.1). The difference is that acyl transfer involves transfer to an acceptor, whereas in hydrolysis the acceptor is water. Acyl transfer is kinetically controlled; the thermodynamically favored product is hydrolysis.

Acyltransferases catalyze critical steps in antibiotic biosynthesis and other pathways such as amino acid biosynthesis.^[1] Both polyketide biosynthesis and non-ribosomal peptide syn-

thesis use acyltransferases to catalyze macrocyclization or acylation, Scheme 2. Macrocyclization reduces the conformational freedom to ensure that the molecule is complementary to biological target and to reduce its susceptibility to proteases. Acylation, usually with a hydrophobic acyl group, of the aglycone or sugar moiety allow the antibiotics to interact with hydrophobic targets such as cell membranes. Acyltransferases also catalyze key steps in amino acid biosynthesis. Homoserine O-acetyltransferase (HTA) from *Haemophilus influenzae* catalyzes the transfer of the acetyl group from acetyl-CoA to l-homoserine to form O-acetylhomoserine Scheme 2.^[2,3]

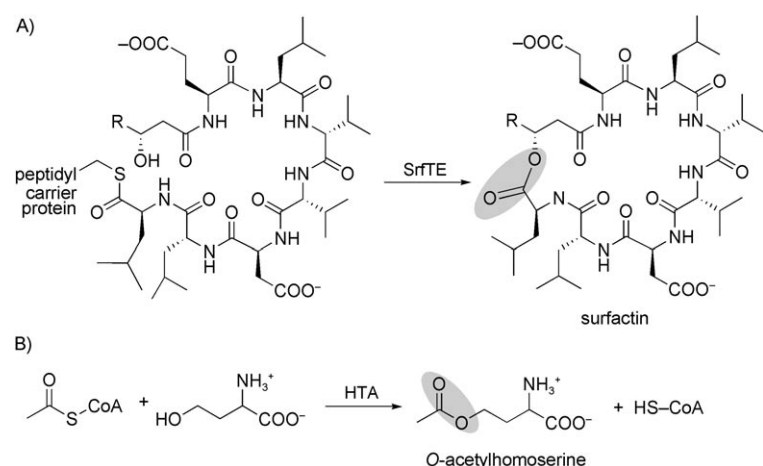
Acyltransferases also catalyze critical steps in the synthesis of bacterial polyesters, triacylglycerols, and wax esters. Many bacteria store excess carbon as insoluble granules of poly- β -hydroxybutyrate. The elongation step of this polyester synthesis involves an acyl transfer of the growing polyester chain to an added monomer.^[4] In triacylglycerol or wax ester synthesis,

[a] Dr. Y. Jiang, Prof. Dr. R. J. Kazlauskas
Department of Biochemistry, Molecular Biology and Biophysics
Biotechnology Institute, University of Minnesota
1479 Gortner Avenue, Saint Paul, MN, 55108 (USA)
Fax: (+1) 612-625-5780
E-mail: rjk@umn.edu

[b] Dr. K. L. Morley
Department of Chemistry, McGill University
Montréal, Québec, H3A 2K6 (Canada)

[c] Dr. J. D. Schrag
National Research Council Biotechnology Research Institute
6100 Royalmount Avenue, Montréal, Québec, H4P 2R2 (Canada)
Fax: (+1) 514-496-5143
E-mail: joe@bri.nrc.ca

Supporting information for this article is available on the WWW under <http://dx.doi.org/10.1002/cbic.201000693>.



Scheme 2. Acyltransferases catalyze key steps in antibiotic and amino acid synthesis. A) Surfactin synthase thioesterase domain (SrfTE) catalyzes intramolecular cyclization of peptidyl carrier protein thioester to form macroactone cyclic heptapeptide. B) As part of methionine biosynthesis homoserine O-acetyltransferase (HTA) catalyzes the transfer of the acetyl group from acetyl-CoA to L-homoserine to form O-acetylhomoserine.

acyltransferases add the acyl group from acyl-coenzyme A to a diacylglycerol to make a triacylglycerol, or to a long-chain alcohol to make a wax ester.^[5] Cholesterol transport and lipoprotein assembly also involves acyltransferases. Inhibitors of N-myristoyltransferase might alleviate sleeping sickness.^[6]

Acyltransferases are also used in biocatalysis for the chemoenzymatic synthesis of natural product analogues. For example, Walsh and co-workers used a cloned thioesterase to catalyze the macrocyclization of peptides to create small libraries of macrolactams.^[7] Such reactions would have yielded mixtures of different cyclization products without an enzyme. Later the same group used a different thioesterase to regioselectively acylate vancomycin or teicoplanin variants.^[8] In another acylation example, Tang's group used the acyltransferase LovD in the gram-scale chemoenzymatic synthesis of simvastatin, a cholesterol-lowering drug that is a semisynthetic analogue of the natural product lovastatin. This procedure allowed the use of water as the solvent and avoided multiple protection and deprotection steps.^[9] Green and co-workers used choline acyltransferases to make potential inhibitors of choline acyltransferases themselves.^[10]

Esterases/lipases and acyltransferases catalyze both hydrolysis and acyl transfer, but esterases/lipases favor hydrolysis (transfer of the acyl group to water), whereas acyltransferases favor transfer to an acceptor other than water. In nonaqueous solvents, esterases and lipases favor acyl transfer to an acceptor over hydrolysis. Lyophilized powders of esterases or lipases suspended in nonaqueous solvents, typically ionic liquids or nonpolar organic solvents, catalyze acyl transfer.^[11] Examples include the resolution of alcohols by enantioselective acylation, regioselective acylation of sugars, and the synthesis of polymers by ring-opening polymerization of lactones.

Hydrolysis is a common side reaction of acyltransferases, especially in the absence of an acceptor. For example, ~30% hydrolysis accompanied the macrocyclization of a natural peptide

catalyzed by Srf TE domain in vitro.^[12] Homoserine acetyltransferase and DEBS TE catalyze hydrolysis of acetyl CoA and N-acetylcysteamine thioester derivatives in the absence of an acceptor.^[3,13] Some in vitro experiments use thioesterases excised from large multidomain complexes and show more hydrolysis than expected. Addition of solvents and surfactants also influences the relative amount of hydrolysis.

This overlapping catalytic activity in esterases/lipases and acyltransferases is due to their similar 3D structures and similar catalytic machinery. Both adopt the α/β -hydrolase fold.^[14] A few esterases and acyltransferases adopt other folds such as the β -lactamase fold adopted by esterase B from *Burkholderia gladioli*^[15] and simvastatin acyltransferase,^[16] but these other folds are not considered in this paper. Both esterases/lipases and acyltransferases in the α/β -hydrolase-fold class contain a Ser-His-Asp(Glu) catalytic triad, an oxyanion hole and follow a ping-pong bi-bi reaction mechanism involving an acyl-serine enzyme intermediate. In both cases, catalysis starts by the serine nucleophile attacking the substrate's

carbonyl carbon and the formation of an acyl-enzyme intermediate. The next step differs in the two enzyme classes: in esterases/lipases: a water nucleophile attacks acyl-enzyme intermediate, whereas in acyltransferases an alcohol nucleophile (or other acyl acceptor) attacks acyl-enzyme intermediate.

Despite the X-ray crystal structures of eight acyltransferases, including structures with bound substrate analogues, the molecular basis of acyltransferase activity versus hydrolysis remains elusive. The key difference between these reactions is choosing between water and alcohol (or amine) as the nucleophile. There are two ways to favor acyltransfer over hydrolysis: first, decrease the ability of water to act as a nucleophile or second, increase the ability of alcohol to act as a nucleophile. Both approaches can work simultaneously. In two cases crystallographers suggested that the active site of acyltransferases is hydrophobic and excludes water (Srf TE, *Mycobacterium* antigens), but in three cases (HiHAT, LiHAT, fengycin TE) crystallographers did not mention any evidence for a water-excluding mechanism. Most structures show evidence for specific interactions between the alcohol and acyltransferase that favor acyltransfer over hydrolysis. However, the alcohol differs for each acyltransferase, so the structural features that favor its binding will also differ. We did not study the alcohol binding contribution to acyltransfer in this paper.

Our hypothesis is that, besides binding the nucleophile, which is specific for each nucleophile, there is also a common mechanism for deactivation of water as a nucleophile in acyltransferases. Our approach is to compare the X-ray crystal structures of related hydrolases and acyltransferases to identify the structural differences, especially in the active-site region that binds the nucleophilic water or alcohol. We found a difference in the main-chain orientation of the oxyanion loop in the active site and propose a mechanism for how this different orientation can deactivate water as a nucleophile.

Results

Structure differences between *Haemophilus influenzae* homoserine acyltransferase (HiHAT) and *Pseudomonas fluorescens* esterase (PFE)

Although the amino acid sequences of HiHAT and PFE differ significantly (only 13% sequence identity), their 3D structures (PDB IDs: 2b61 and 1va4, respectively) are very similar. The Z-score for the structural overlay by using DALI^[17] is 23.8 and root-mean-square deviation between the atoms in the two structures is 3.1 Å over 257 amino acids.

The major difference in the active sites is the oxyanion loop conformation. This loop occurs after strand β_3 in the α/β -hydrolase fold and contains one residue that donates a main-chain NH to stabilize the oxyanion intermediate during catalysis. This residue, called the first oxyanion residue in this paper, is Leu49 in HiHAT and Trp28 in PFE. In HiHAT this loop adopts a type-I β -turn, whereas in PFE it adopts a type-II β -turn.

β -Turns reverse the direction of the peptide chain and consist of four amino acid residues; the first and last residues (i and $i+3$) form a hydrogen bond between C=O (i) to NH ($i+3$),^[18] Figure 1. This hydrogen bond is similar to the one be-

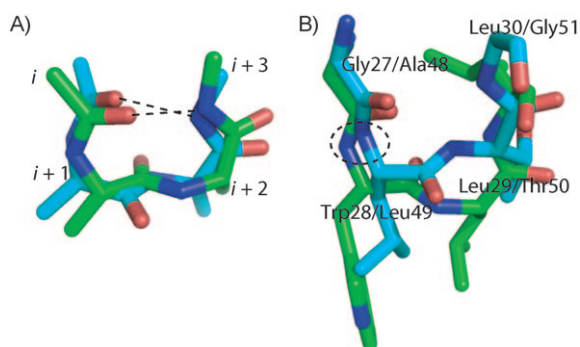


Figure 1. β -turns. A) Idealized type-I β -turn (cyan carbons) overlaid on an idealized type-II β -turn (green carbons). The amino acids are XxxAlaAlaXxx, where Xxx indicates an incompletely specified residue since only part of the i and $i+3$ residues are shown. The labels are near the C_{α} of each residue; dotted lines indicate hydrogen bonds between the carbonyl of residue i and the NH of residue $i+3$. B) Superimposed X-ray crystal structures of the oxyanion loop regions of PFE (green carbons, a type-II β -turn) and HiHAT (cyan carbons, a type-I β -turn). The structures were superimposed by pair fitting of the active site serine and histidine (not shown in Figure for clarity). In this view, the active site lies behind the plane of the paper so the carbonyl of $i+1$ in PFE (green) points toward the active site, whereas for HiHAT (cyan carbons) the carbonyl of $i+1$ points away from the active site. In both cases the NH of $i+1$ (circled with a dashed line) points toward the active site because it forms a hydrogen bond with the oxyanion intermediate.

tween adjacent antiparallel β strands; hence the name β -turn. The two central residues in a β -turn (second and third residues called $i+1$ and $i+2$, respectively) lack hydrogen bonds between the main-chain carbonyl and NH groups. This lack of hydrogen bond is critical for catalysis in ester hydrolysis and acyl transfer because the $i+1$ NH group stabilizes the oxyanion intermediate by donating a hydrogen bond.

The central residues in a β -turn can adopt different conformations. The type-I β -turn contains $\Phi_{i+1} = -60^\circ$, $\psi_{i+1} = -30^\circ$, $\Phi_{i+2} = -90^\circ$, $\psi_{i+2} = 0^\circ$, whereas the type-II β -turn contains $\Phi_{i+1} = -60^\circ$, $\psi_{i+1} = 120^\circ$, $\Phi_{i+2} = 80^\circ$, $\psi_{i+2} = 0^\circ$. Conformations can vary within $\pm 30^\circ$ of these ideal values. In PFE these angles are -66° , 135° , 87° , -21° and thus correspond to a type-II turn ($i+1 = \text{Trp28}$, $i+2 = \text{Leu29}$). In HiHAT, these angles are -48° , -49° , -109° , 14° and correspond to a type-I turn ($i+1 = \text{Leu49}$, $i+2 = \text{Thr50}$). The consequence of this difference is that the carbonyl groups of PFE Trp28 and HAT Leu49 point in opposite directions: PFE Trp28 carbonyl points into the active site, whereas HAT Leu49 carbonyl points away from the active site.

Different oxyanion loop conformation in GX-class hydrolases versus acyltransferases

We hypothesize that this difference in oxyanion turn orientation for PFE and HiHAT is a common feature that distinguishes esterases from acyltransferases. To test this hypothesis we made a more extensive comparison of structures within closely related esterases/lipases and acyltransferases. For the hydrolases, we focused on esterases/lipases within the α/β -hydrolase superfamily, and further narrowed our comparison to those with a GX-class oxyanion loop. The lipase engineering database subdivides lipases according to the oxyanion loop orientation into GX, GGGX, and Y classes,^[19] in which G represents glycine, X represents any amino acid, and Y represents tyrosine. The oxyanion loop orientation in acyltransferases (see below) is similar to GX family hydrolases, but the other two classes have significantly different orientations of the oxyanion loops. The GGGX class has a much larger space, whereas the Y class uses the tyrosine side chain to stabilize the oxyanion so that the main-chain orientation differs significantly. As mentioned above, we excluded any structures such as closed conformations of lipases in which there was doubt as to whether it was a catalytically active conformation. We included all hydrolases in the structural classification of proteins (SCOP) database^[20] that fit these criteria. We found thirty-two X-ray structures of hydrolases that fit these criteria; these are listed in Table S1 in the Supporting Information.

The oxyanion loop in most of these hydrolases adopts a type-II β -turn and all but one point the carbonyl group of the $i+1$ residue toward the active site, Table S1. Among thirty-two GX-class hydrolases, twenty-one have angles are within 30° of the ideal values defined above for type-II β -turns, three have angles deviate slightly more than 30° from the ideal values, seven are not type-II β -turn because the last two angles (Φ_{i+2} , ψ_{i+2}) deviate significantly from those for a type-II β -turn. In all thirty-one of these structures, the first two dihedral angles in the definition of a type-II β -turn (Φ_{i+1} , ψ_{i+1}) are similar. The Φ_{i+1} angles range between -82° and -44° and the ψ_{i+1} angles range between 112° and 155° . Because of this similarity in the dihedral angles for $i+1$, the carbonyl group of this residue points toward the active site in all thirty-one structures. The backbone NH of this residue, whose catalytic role is stabilization of the oxyanion, also points toward the active site. The

one exception to this generalization is human fatty acid synthetase thioesterase domain, which shows a type-I β -turn for the oxyanion turn^[21] This exception is rationalized in the Supporting Information.

Acyltransferases fall into several superfamilies within the SCOP database, but only acyltransferases that have the α/β -hydrolase fold are included in this comparison. For example, homoserine O-succinyl transferase from *Bacillus cereus* (PDB ID: 2ghr) is not included because its structure belongs to the class-I glutamine amidotransferase-like superfamily. Similarly, histone acetylases are not included because most structures belong to the acyl-CoA N-acyltransferases superfamily. Three acyltransferases within the α/β -hydrolase fold superfamily are not included in Table S2 because their oxyanion loops are distorted. Two thioesterases of polyketide biosynthesis (erythromycin thioesterase and pikromycin thioesterase) contain a two-residue insertion in the oxyanion loop, which significantly changes its orientation, see the Supporting Information for details. Myristoyl-ACP-specific thioesterase is also excluded because the X-ray structure^[22] did not definitively identify the oxyanion loop. The most likely oxyanion loop is too far from the active site: 8.6 Å from O γ of Ser114 to the backbone nitrogen of Phe44. (The corresponding distance in PFE is 4.8 Å.) Catalysis might require a conformational change or a bridging water molecule. Table S2 lists the eight acyltransferases in the α/β -hydrolase fold superfamily that fit our criteria. These include three mycolyl transferases (*Mycobacterium tuberculosis* antigens), two thioesterases from polyketide antibiotic biosynthesis that catalyze cyclization of surfactin or fengycin, two homoserine acyltransferases and an acetyl transferase from the β -lactam antibiotic biosynthesis.

The oxyanion turns in all eight acyltransferases in Table S2 are either type-I β -turns or very close to a type-I β -turn. In particular, the dihedral angles of the oxyanion residue are similar in each case: the Φ_{i+1} angles range from -70° to -46° and the ψ_{i+1} angles range from -52° to -24° . The conformation of the oxyanion residues maintains the catalytically essential NH in position to hydrogen bond to the oxyanion intermediate. However, this conformation points the carbonyl oxygen of this residue away from the active site. This different orientation of the carbonyl group is the major structural difference between hydrolases and acyltransferases.

A graphic comparison of conformations of the oxyanion residue ($i+1$ of the β -turn) shows a dramatic difference between the hydrolases and the acyltransferases, Figure 2. The Φ_{i+1} angles are similar for both: an average of $-62 \pm 8^\circ$ for the hydrolases in Table S1 (excluding hydrolase 1xkt) and average of $-54 \pm 8^\circ$ for the acyltransferases in Table S2. This similarity places the backbone amide NH and the C α of $i+1$ in similar orientations and allows this amide NH to contribute to catalysis in both classes of enzymes. In contrast, the ψ_{i+1} angles differ. For hydrolases, this angle averages $134 \pm 9^\circ$, whereas for acyltransferases it averages $-40 \pm 10^\circ$. This 174° difference corresponds to an opposite orientation for the carbonyl oxygen of this residue.

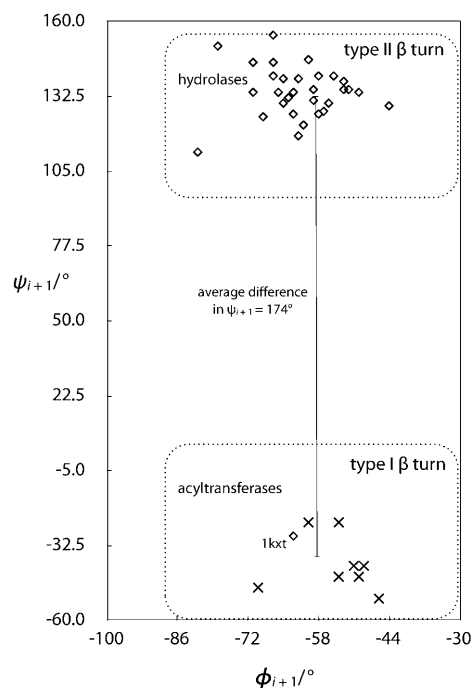
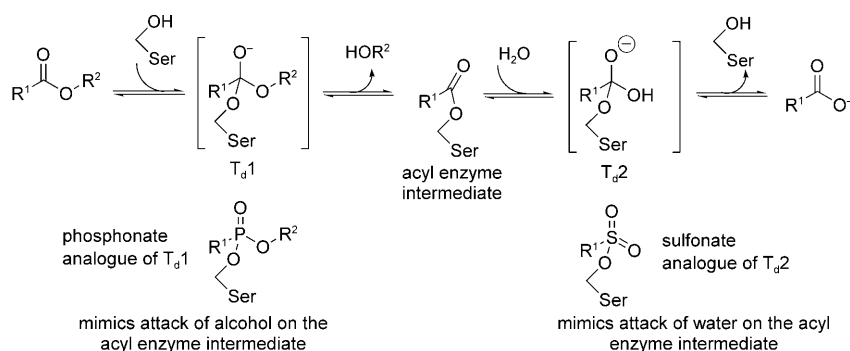


Figure 2. Dihedral angles of the oxyanion residue ($i+1$ in the turn) in hydrolases and acyltransferases. The hydrolases (diamonds) have $\Phi_{i+1} = -62 \pm 8^\circ$, $\psi_{i+1} = 134 \pm 9^\circ$, which points the carbonyl oxygen of these residues toward the active site. The acyltransferases (crosses) have $\Phi_{i+1} = -54 \pm 8^\circ$, $\psi_{i+1} = -40 \pm 10^\circ$, which points the carbonyl oxygen of these residues away from the active site. The average difference in ψ_{i+1} is 174° , which corresponds to an opposite orientation for the carbonyl oxygen of these residues. One hydrolase, labeled 1xkt, lies among the acyltransferases and is not included in the averages. The Supporting Information suggests an explanation for this exception. The dotted lines indicate angles within 30° of the ideal values for β -turns. (This Figure shows that the dihedral angles of the oxyanion residue are in the range for a type-II β -turn for 30 of the 31 hydrolases. Only 23 of the 31 hydrolases also have the dihedral angle for the next amino acid residue in the range for a type-II β -turn. The orientation of the next amino acid does not affect orientation of the key carbonyl oxygen.)

X-ray crystal structure of a sulfonate transition-state analogue bound to PFE to mimic hydrolysis

The key difference between hydrolysis and acyl transfer is the choice between water or alcohol as the nucleophile. A phosphonate transition-state analogue mimics the attack of alcohol on the acyl-enzyme, whereas a sulfonate transition-state analogue mimics the attack of water on the acyl-enzyme. Phosphonates contain an -OR moiety that mimics the alcohol of the ester, whereas sulfonates contain a sulfonyl oxygen to mimic the attacking water, Scheme 3. Crystallographers have solved many X-ray crystal structures of lipases and esterases containing bound phosphonate transition-state analogues, but not of a sulfonate transition-state analogue bound to a GX-class hydrolase. For this reason, we synthesized butane-2-sulfonic acid 4-nitrophenyl ester as an irreversible inhibitor of PFE and solved its X-ray crystal structure bound to PFE. (Two previous X-ray structures of a sulfonate transition-state analogues bound to an esterase^[23] are catalytically not productive orientations because some of the key hydrogen bonds are missing, or the transition-state analogue orients in with the acyl mimic in



Scheme 3. Mechanism for hydrolysis of an ester, $R^1C(O)OR^2$, by a serine esterase. Attack of the serine on the ester forms the first tetrahedral intermediate, T_{d1} . A phosphonate linked to the serine mimics this first intermediate. The R^1 on the phosphonate corresponds to the R^1 on the acyl part of the ester and R^2 on the phosphonate corresponds to the R^2 on the alcohol part of the ester. Loss of the alcohol, HOR^2 , from T_{d1} gives the acyl-enzyme intermediate. Attack of water on the acyl-enzyme forms the second tetrahedral intermediate, T_{d2} . A sulfonate linked to the serine mimics this second tetrahedral intermediate. The R^1 on the sulfonate corresponds to R^1 on the acyl part of the ester. One of the sulfonate oxygens mimics the oxyanion oxygen of T_{d2} , and the other sulfonate oxygen mimics the attacking water of T_{d2} . Loss of the serine from T_{d2} gives the product acid. For simplicity, the drawing omits protonation and deprotonation steps.

the alcohol region.) Details of the crystallization, data collection, and refinement are in the Supporting Information.

Alignment of the complex and wild-type structures reveals only minor changes to the active site. The 2-butyl substituent points toward the solvent, Figure 3. Detailed analysis of this orientation and implications for enantioselectivity will be reported elsewhere. The inhibitor mimics a catalytically productive orientation because it contains all of the five hydrogen bonds necessary for catalysis. The sulfonyl oxygen in the oxyanion hole is hydrogen bonded to the NH of both Met95 and Trp28 (2.9 and 3.0 Å, respectively), whereas the second sulfonyl oxygen is weakly hydrogen bonded to His251 Nε2 (3.3 Å) and to the bridging water molecule (3.2 Å). The unit cell contains six protein molecules; chains A and D show this bridging water molecule, while the other chains do not, likely due to disorder. This bridging water molecule also hydrogen bonds to the main-chain carbonyl oxygen of Trp28 (2.5 Å). The catalytic Ser94 Oγ is hydrogen bonded to the His251 Nε2 (3.2 Å) and Asp222 Oδ2 is hydrogen bonded to His251 Nδ1 (2.8 Å; also not shown in Figure 3 for clarity). Figure 3B shows a schematic of the hydrogen bonds between the sulfonate transition-state analogue and the protein, whereas panel C shows how these hydrogen bonds would look in the tetrahedral intermediate during hydrolysis. The X-ray crystal structure does not reveal the positions of the hydrogen atoms; all hydrogen bonds are inferred from the close distances of the oxygen or nitrogen atoms.

To confirm that the water molecule bridging the sulfonyl transition-state analogue and the oxyanion loop is stable at that location, we used a molecular dynamics simulation (Figure 4). By starting from the X-ray crystal structure (subunit D) placed in a box of water molecules, molecular dynamics simulated movement of the complex for 1.2 ns. The bridging water molecule remained in position and maintained the two hydrogen bonds (average O–O distance ~2.9 Å).

In the case of attack of water on an acyl-enzyme intermediate, this bridging water interaction is expected to be stronger than it is for the sulfonyl transition-state analogue. The bridging water molecule will not interact with a sulfonyl oxygen, but rather with an attacking water molecule. The oxygen of this water molecule will be more negatively charged than a sulfonyl oxygen because the active-site histidine acts as base to deprotonate it.

An X-ray crystal structure of a sulfonate transition-state analogue bound to an acyltransferase (fengycin thioesterase) un-

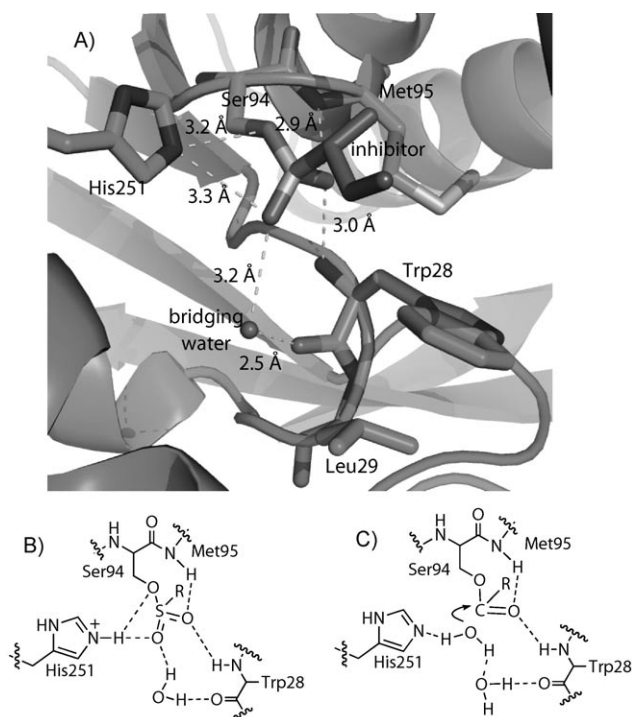


Figure 3. X-ray crystal structure of a sulfonate transition-state analogue bound to the catalytic serine of esterase from *Pseudomonas fluorescens* suggests a mechanistic role for a main-chain carbonyl oxygen of the oxyanion loop. A) The active site of PFE showing key hydrogen bonds to the sulfonate transition-state analogue covalently linked to Ser94. One sulfonyl oxygen, partly obscured by the R group of the sulfonate in this view, mimics the oxyanion oxygen and accepts hydrogen bonds from the main-chain NH of Met95 and Trp28 (2.9 and 3.0 Å, respectively). Another sulfonyl oxygen mimics the attacking water molecule and accepts hydrogen bonds from the catalytic His251 and a bridging water molecule (ball; 3.3 and 3.2 Å, respectively). This bridging water molecule also hydrogen bonds to the main-chain carbonyl oxygen of tryptophan 28 (2.5 Å). B) A schematic diagram of the X-ray crystal structure in panel A showing the hydrogen bonding pattern. C) Schematic diagram of the tetrahedral intermediate that corresponds to the sulfonate mimic in panel A and B. The attacking water molecule (bonded to the reacting carbon) makes hydrogen bonds to both the active site His251 and the bridging water molecule.

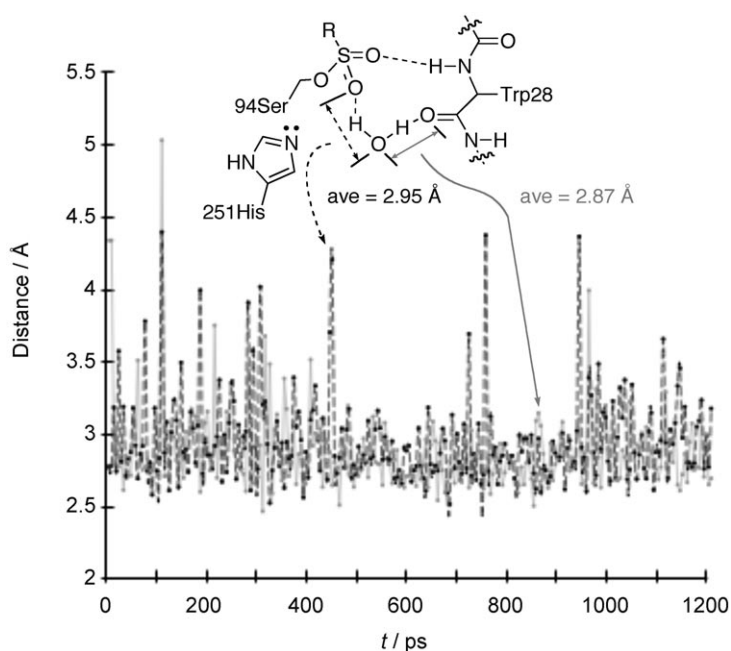


Figure 4. Molecular dynamics simulation of a bound water molecule in the active site of PFE. The X-ray crystal structure of some subunits showed a water bridging from the transition-state analogue to the oxyanion loop with hydrogen bonds. The molecular dynamics simulation follows these hydrogen bonds. The distances from the bound water to the sulfonyl transition-state analogue oxygen (shown in black, average value is 2.95 Å) and Trp28 carbonyl oxygen (shown in gray, average value is 2.87 Å) remain near 2.9 Å, which indicates stable hydrogen bonds.

fortunately shows a catalytically nonproductive orientation and thus, provides little insight into the mechanism.^[24] Fengycin thioesterase catalyzes the macrocyclization of a peptide, but the transition-state analogue was phenylmethylsulfonyl fluoride. The phenylmethylsulfonyl moiety bound to the active-site serine, but imperfectly mimicked the transition state, likely because the phenylmethyl moiety imperfectly mimicked the substrate peptide. One sulfonyl oxygen formed the expected two hydrogen bonds in the oxyanion hole, but the active-site histidine adopted a catalytically non-productive orientation. A bridging water molecule accepted a hydrogen bond from the NH of the oxyanion loop (Ser31; N–O distance 3.3 Å). The bridging water molecule did not donate a hydrogen bond the sulfonate oxygen, which mimics the attacking water (O–O distance 4.2 Å). One can conclude that a bridging water molecule likely exists in the active site during catalysis by this acyltransferase, but one cannot say anything about its role in catalysis.

Mechanistic significance of the type-I versus type-II orientation of the oxyanion turn

The interaction with the bridging water molecule might contribute to catalysis, Figure 5. In a hydrolase, the bridging water molecule could act as a base by accepting a hydrogen bond from the attacking water molecule. This additional basic interaction could increase the reactivity of the attacking water molecule. The role of the active-site histidine as a base is well established; the current proposal is that the bridging water mol-

ecule can act as an additional base. Although in principle, a water molecule can be either a hydrogen-bond donor or acceptor, the interaction of this bridging water molecule with the carbonyl oxygen of Trp28 sets its role as a base. The carbonyl oxygen of Trp28 can only accept a hydrogen bond, and thus, the bridging water donates a hydrogen bond. Because its partial negative charge has increased, the bridging water molecule will now accept a hydrogen bond from the attacking water. Another role for the bridging water molecule during hydrolysis might be to aid positioning the attacking water molecule in a catalytically productive orientation.

In contrast to acyl transferases, the bridging water molecule in acyltransferases might hinder the hydrolysis step. First, the carbonyl in hydrolases and the NH in acyltransferases are in slightly different locations, which places the bridging water molecule further from the serine in acyltransferases than in hydrolases. The bridging water molecule might be too far away to interact with the attacking water molecule or it might position the attacking water molecule too far from the carbonyl carbon to attack effectively. Second, the NH donates a hydrogen bond to the bridging water so that it, in turn, can donate a hydrogen bond to the attacking water, Figure 5. This acidic interaction decreases the nucleophilicity of the attacking water and might slow down hydrolysis.

Finally, during acyl transfer in acyl transferases, the bridging water molecule has no effect. The acceptor alcohol or amine displaces the bridging water molecule from the active site, so it does not aid or hinder catalysis, Figure 5. The acceptors are larger than a water molecule and therefore displace the bridging water molecule. X-ray crystal structures of phosphonates bound to the active site of both hydrolases (e.g., *Burkholderia cepacia* lipase,^[25] *Pseudomonas aeruginosa* lipase,^[26] *Bacillus subtilis* lipase A,^[27] dog gastric lipase^[28]) and *Rhizomucor miehei* lipase^[29]) and acyltransferases (e.g., *Mycobacterium antigen*^[30]) show either no water molecule or a water molecule that is too far to form a hydrogen bond to the alcohol oxygen.

Discussion

Other crystal structures of hydrolases have also identified secondary base interactions to the attacking water molecule including several that involve a bridging water molecule. In the glutamic peptidase family, the hydrolytic water hydrogen bonds to the catalytic glutamate base and to the carbonyl oxygen O ϵ 1 of a nearby glutamine.^[31] In a glycoside hydrolase, the hydrolytic water hydrogen bonds with both the catalytic aspartate and an adjacent tyrosine phenolic oxygen that helps position the water molecule.^[32] Three examples involve a bridging water molecule. Potato epoxide hydrolase and haloalkane dehalogenase, which both have the same α/β -hydrolase fold as esterases and acyltransferases, show a bridging interaction that is the same as the one proposed for esterases in the current paper. In epoxide hydrolase, a bridging water molecule

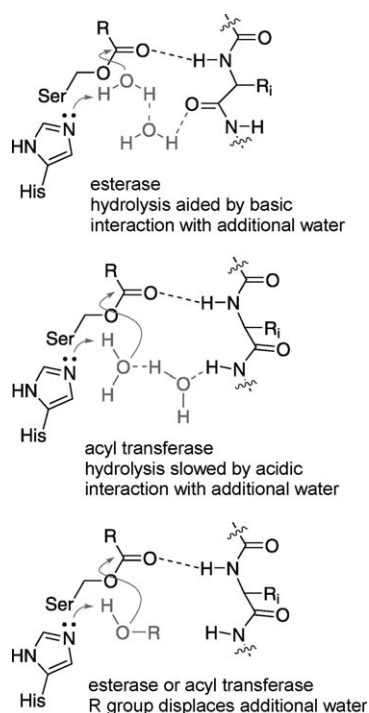


Figure 5. Hypothesis for how the different conformation of the oxyanion loop in esterases and acyltransferases can activate or deactivate the attacking water via a second water molecule. In esterases, the main-chain carbonyl oxygen acts as a base via a bridging water molecule to activate the attacking water molecule. In acyltransferases, the NH acts as an acid via a bridging water molecule to deactivate the attacking water molecule. For the acyl transfer reaction, the attacking nucleophile is an alcohol, which is larger than water. This alcohol displaces the bridging water molecule thereby eliminating any activating or deactivating effects.

hydrogen bonds to the main-chain carbonyl oxygen of Phe33 and the attacking water,^[33] whereas in the haloalkane dehalogenase this bridge is between main-chain carbonyl oxygen of Asn38 and the attacking water.^[34] In the second case, molecular dynamics simulations also suggest that this bridging water molecule has an important role in catalysis. In a penicillinase, the attacking water hydrogen bonds to both the base (O γ of Ser87) and a bridging water molecule linked to O γ of Ser110.^[35] Recent modeling and mutagenesis indicated that a water network contributes to the amidase activity of a *Bacillus* esterase.^[36] Using a bridging water molecule in addition to the hydrolytic water molecule is disfavored by entropy, but the enthalpic advantage of the hydrogen bonds formed likely compensate for the entropic cost.^[37]

Secondary base interaction is not essential for hydrolases activity because some hydrolases show no evidence of a secondary base interaction. One previous X-ray crystal structure of a lipase did contain a sulfonate transition-state analogue,^[38] but this was not a GX-class hydrolase. *Candida rugosa* lipase belongs to the GGGX class of lipases, the oxyanion loop of which is farther from the active-site serine and tetrahedral intermediate to interact with them directly or by way of a bridging water molecule. There was no evidence of a bridging water molecule in this structure, so the proposed secondary base interaction might not be essential for catalysis. Several serine

proteases are a second example of hydrolases that show no secondary base interaction. The X-ray crystal structures proteases of acyl-enzyme intermediates in several serine proteases have identified the likely hydrolytic water.^[39] This water hydrogen bonds to N ϵ 2 of the catalytic histidine, but not to anything else.

Other hydrolases can use alternative mechanisms to activate water. Lipase from *Candida antarctica* has a water tunnel that connects the solvent to the active site. Blocking this tunnel by site-directed mutagenesis decreased the relative amount of hydrolysis versus transesterification by approximately sixfold.^[40] This tunnel mechanism could be more important for lipases, which might be partly buried in a lipid during catalysis. Subtilisins also contain a water tunnel.^[41]

If a secondary base interaction can activate a water for reaction, then a secondary acid interaction should deactivate a water for reaction. In acyltransferases the oxyanion turn orients the central amide bond in an opposite manner so an NH, not a carbonyl oxygen point toward the active site. Although no structural information is available on the attacking water molecule in these enzymes, we hypothesize that the situation is similar to GX-class hydrolases. However, the NH donates a hydrogen bond to the bridging water, which in turn donates a hydrogen bond to the attacking water. This donation of a hydrogen decreases the nucleophilicity of the attacking water. This interaction could be partly responsible for the different chemical reactivity of the hydrolases versus acyltransferases.

Alternative hypotheses for the significance of the different oxyanion loop orientation to the hydrolase versus acyltransferase mechanism are possible. For example, the different oxyanion loop orientation points the dipole of the carbonyl in different directions in hydrolases and acyltransferases. The strength of our work is to identify the structural difference between the two classes of enzymes. Our suggestions for the role of the bridging water molecule are consistent with the known structure and mechanisms, but it does not rule out alternative explanations.

Previous research had identified that the oxyanion loop can contribute the preference for acyl transfer, but had not identified how. Site-directed mutagenesis in the oxyanion loop of surfactin thioesterase increased the relative amount of hydrolysis over acyl transfer.^[12] Wild-type enzyme showed 71% acyl transfer, but the Pro29Gly variant showed only 23% acyl transfer, the rest was hydrolysis. This amino acid substitution likely changed the conformation of the oxyanion turn due to the different conformational preferences of proline versus glycine, but the nature of the conformational change was not established. In cyclization reactions, the higher effective molarity of the nucleophile due to the folded conformation of peptide or polyketide can favor acyl transfer over hydrolysis, but many acyl transfers do not involve cyclization.

Stehle and co-workers^[42] made homology models of plant acyltransferases^[43] but, after careful analysis, concluded that "there is no reliable explanation" for the reactivity differences between hydrolases and acyltransferases. The homology models were based on hydrolases and thus contained a hydrolase-like oxyanion loop orientation. Our proposed molecular

basis involves main-chain interactions, which are difficult to find by using amino acid sequence comparisons. There is no clear link between amino acid sequence and the types-I or II conformation in a β -turn. For this reason, a bioinformatics approach would not identify sequence motifs characteristic of hydrolases or acyltransferases. We previously identified the importance of main-chain interactions for perhydrolysis activity.^[44] Moving the same oxyanion loop closer to the active site could create a perfect fit for hydrogen peroxide and thus, enhance perhydrolysis.

Experimental Section

(±)-Butane-2-sulfonic acid 4-nitrophenyl ester: (*S*)-*sec*-butyl ethanethioate^[45] was oxidized to the sulfonic acid and isolated as the sodium salt. Chlorination with thionyl chloride and addition of *p*-nitrophenol and Et₃N yielded the desired *p*-nitrophenyl sulfonate ester. The Supporting Information contains synthetic details.

X-ray crystal structure of (±)-butane-2-sulfonyl bound to PFE: Incubation of wild-type PFE for 24 h with a tenfold excess of (±)-butane-2-sulfonic acid 4-nitrophenyl ester inhibited 95% of the hydrolytic activity. The PFE-inhibitor complex and mutants formed single crystals under conditions similar to those for wild-type PFE.^[46] 1.7 M (NH₄)₂SO₄, 3% PEG 400 in 0.1 M NaKH₂PO₄ pH 7.5. The PFE-inhibitor complex crystals were isomorphous with those for wild-type PFE (PDB ID: 1va4). The structure is high quality ($R_{\text{work}} = 19.8\%$, $R_{\text{free}} = 20.7\%$) with a resolution of 1.65 Å, Table S3 in the Supporting Information and PDB ID: 3ia2. The structure showed only the *R* enantiomer of the sulfonyl, even though the inhibitor was racemic. This *R* enantiomer corresponds the fast reacting enantiomer of the corresponding ester substrate methyl (*R*)-2-methylbutanoate.^[47] PFE favors the *R* enantiomer of the ester 32-fold over the *S* enantiomer and it is likely that PFE shows a similar enantioselectivity toward the nitrophenyl sulfonate enantiomers.

Molecular dynamics simulation: Starting from the D subunit of the X-ray crystal structure of PFE containing the covalently bound sulfonate (PDB ID: 3ia2), protons were added by using the protein preparation wizard of Maestro (Schrödinger LLC). By using the software Desmond (D.E. Shaw Research, New York, NY), the protein was placed in a box (69×69×69 Å) of water molecules (SPC model^[48]) with 27 sodium cations and 20 chloride anions to neutralize the charge. The system was initially minimized by using the OLPS2005 force field^[49] followed by several steps of equilibration by using Berendsen thermostat and barostat method.^[50] The simulation (300 K, 1 atm pressure) by using Desmond for 1.2 ns with a step time of 1 fs and recorded every 4.8 ps. The Coulomb interaction was cutoff at 15 Å and the long-range electrostatic interaction was calculated with particle mesh Ewald (PME) method.

Acknowledgements

We thank the University of Minnesota, the Institute for Renewable Energy and the Environment (University of Minnesota) and Natural Sciences and Engineering Research Council (Canada) for financial support. We thank the Minnesota Supercomputing Institute for access to computers and molecular modeling software and Dr. Nicholas Labello for help with the molecular dynamics simulation.

Keywords: hydrolases · oxyanion loops · structure–activity relationships · transferases · X-ray diffraction

- [1] J. Grünwald, M. A. Marahiel, *Microbiol. Mol. Biol. Rev.* **2006**, *70*, 121–146; F. Kopp, M. A. Marahiel, *Nat. Prod. Rep.* **2007**, *24*, 735–749.
- [2] I. A. Mirza, I. Nazi, M. Korczynska, G. D. Wright, A. M. Berghuis, *Biochemistry* **2005**, *44*, 15768–15773.
- [3] T. L. Born, M. Franklin, J. S. Blanchard, *Biochemistry* **2000**, *39*, 8556–8564.
- [4] J. Stubbe, J. Tian, A. He, A. J. Sinskey, A. G. Lawrence, P. Liu, *Ann. Rev. Biochem.* **2005**, *74*, 433–480.
- [5] M. Wältermann, T. Stöveken, A. Steinbüchel, *Biochimie* **2007**, *89*, 230–242.
- [6] J. A. Frearson, S. Brand, S. P. McElroy, L. A. T. Cleghorn, O. Smid, L. Stojanovski, H. P. Price, M. L. S. Guther, J. S. Torrie, D. A. Robinson, I. Hallyburton, C. P. Mpamhanga, J. A. Brannigan, A. J. Wilkinson, M. Hodgkinson, R. Hui, W. Qiu, O. G. Raimi, D. M. F. van Aalten, R. Brenk, I. H. Gilbert, K. D. Read, A. H. Fairlamb, M. A. J. Ferguson, D. F. Smith, P. G. Wyatt, *Nature* **2010**, *464*, 728–732.
- [7] J. W. Trauger, R. M. Kohli, H. D. Mootz, M. A. Marahiel, C. T. Walsh, *Nature* **2000**, *407*, 215–218; R. M. Kohli, M. D. Burke, J. Tao, C. T. Walsh, *J. Am. Chem. Soc.* **2003**, *125*, 7160–7161.
- [8] R. G. Kruger, W. Lu, M. Oberthür, J. Tao, D. Kahne, C. T. Walsh, *Chem. Biol.* **2005**, *12*, 131–140.
- [9] X. Xie, K. Watanabe, W. A. Wojcicki, C. C. C. Wang, Y. Tang, *Chem. Biol.* **2006**, *13*, 1161–1169; X. Xie, Y. Tang, *Appl. Environ. Microbiol.* **2007**, *73*, 2054–2060.
- [10] K. D. Green, M. Fridman, S. Garneau-Tsodikova, *ChemBioChem* **2009**, *10*, 2191–2194.
- [11] U. T. Bornscheuer, R. J. Kazlauskas, *Hydrolases in Organic Synthesis: Regio- and Stereoselective Biotransformations*, 2nd ed., Wiley-VCH, Weinheim, **2009**, Chapter 5.
- [12] C. C. Tseng, S. D. Bruner, R. M. Kohli, M. A. Marahiel, C. T. Walsh, S. A. Sieber, *Biochemistry* **2002**, *41*, 13350–13359.
- [13] K. K. Sharma, C. N. Boddy, *Bioorg. Med. Chem. Lett.* **2007**, *17*, 3034–3037.
- [14] D. L. Ollis, E. Cheah, M. Cygler, B. Dijkstra, F. Frolow, S. M. Franken, M. Harel, S. J. Remington, I. Silman, J. Schrag, J. L. Sussman, K. H. Verschuere, *Prot. Eng.* **1992**, *5*, 197–211; M. Holmquist, *Curr. Protein. Pept. Sci.* **2000**, *1*, 209–235.
- [15] U. G. Wagner, E. I. Petersen, H. Schwab, C. Kratky, *Prot. Sci.* **2002**, *11*, 467–478.
- [16] X. Gao, X. Xie, I. Pashkov, M. R. Sawaya, J. Laidman, W. Zhang, R. Cacho, T. O. Yeates, Y. Tang, *Chem. Biol.* **2009**, *16*, 1064–1074.
- [17] L. Holm, J. Park, *Bioinformatics* **2000**, *16*, 566–567.
- [18] G. D. Rose, L. M. Gierasch, J. A. Smith, *Adv. Prot. Chem.* **1985**, *37*, 1–109; T. E. Creighton, *Proteins: Structure and Molecular Properties*, 2nd ed., pp. 225–227, Freeman, New York, **1993**; C. M. Wilmot, J. M. Thornton, *J. Mol. Biol.* **1988**, *203*, 221–232.
- [19] J. Pleiss, M. Fisher, M. Peiker, C. Thiele, R. D. Schmid, *J. Mol. Catal. B* **2000**, *10*, 491–508; M. Fischer, J. Pleiss, *Nucleic Acids Res.* **2003**, *31*, 319–321.
- [20] A. G. Murzin, S. E. Brenner, T. Hubbard, C. Chothia, *J. Mol. Biol.* **1995**, *247*, 536–540.
- [21] B. Chakravarty, Z. Gu, S. S. Chirala, S. J. Wakil, F. A. Quiocho, *Proc. Natl. Acad. Sci. USA* **2004**, *101*, 15567–15572.
- [22] D. M. Lawson, U. Derewenda, L. Serre, S. Ferri, R. Sztitner, Y. Wei, E. A. Meighen, Z. S. Derewenda, *Biochemistry* **1994**, *33*, 9382–9388.
- [23] K. K. Kim, H. K. Song, D. H. Shin, K. Y. Hwang, S. Choe, O. J. Yoo, S. W. Suh, *Structure* **1997**, *5*, 1571–1584; K. H. Nam, S.-J. Kim, A. Priyadarshi, H. S. Kim, K. Y. Hwang, *Biochem. Biophys. Res. Commun.* **2009**, *389*, 247–250.
- [24] S. A. Samel, B. Wagner, M. A. Marahiel, L. O. Essen, *J. Mol. Biol.* **2006**, *359*, 876–889.
- [25] A. Mezzetti, J. D. Schrag, C. S. Cheong, R. J. Kazlauskas, *Chem. Biol.* **2005**, *12*, 427–437.
- [26] M. Nardini, D. A. Lang, K. Liebeton, K. E. Jaeger, B. W. Dijkstra, *J. Biol. Chem.* **2000**, *275*, 31219–31225.

- [27] M. J. Dröge, Y. L. Boersma, G. van Pouderoyen, T. E. Vrenken, C. J. Rueggeberg, M. T. Reetz, B. W. Dijkstra, W. J. Quax, *ChemBioChem* **2006**, *7*, 149–157.
- [28] A. Roussel, N. Miled, L. Berti-Dupuis, M. Riviere, S. Spinelli, P. Berna, V. Gruber, R. Verger, C. Cambillau, *J. Biol. Chem.* **2002**, *277*, 2266–2274.
- [29] U. Derewenda, A. M. Brzozowski, D. M. Lawson, Z. S. Derewenda, *Biochemistry* **1992**, *31*, 1532–1541.
- [30] D. R. Ronning, T. Klabunde, G. S. Besra, V. D. Vissa, J. T. Belisle, J. C. Sacchettini, *Nat. Struct. Biol.* **2000**, *7*, 141–146.
- [31] B. Pillai, M. M. Cherney, K. Hiraga, K. Takada, K. Oda, M. N. G. James, *J. Mol. Biol.* **2007**, *365*, 343–361.
- [32] T. Collins, D. De Vos, A. Hoyoux, S. N. Savvides, C. Gerday, J. van Beeumen, G. Feller, *J. Mol. Biol.* **2005**, *354*, 425–435.
- [33] A. Thomaus, J. Carlsson, J. Åqvist, M. Widersten, *Biochemistry* **2007**, *46*, 2466–2479.
- [34] A. Negri, E. Marco, J. Damborsky, F. Gago, *J. Mol. Graphics Modell.* **2007**, *26*, 643–651.
- [35] G. Nicola, S. Peddi, M. E. Stefanova, R. A. Nicholas, W. G. Gutheil, C. Davies, *Biochemistry* **2005**, *44*, 8207–8217.
- [36] R. Kourist, S. Bartsch, L. Fransson, K. Hult, U. T. Bornscheuer, *ChemBioChem* **2008**, *9*, 67–69.
- [37] Z. Li, T. Lazaridis, *Phys. Chem. Chem. Phys.* **2007**, *9*, 573–581.
- [38] P. Grochulski, F. Bouthillier, R. J. Kazlauskas, A. N. Serreji, J. D. Schrag, E. Ziomek, M. Cygler, *Biochemistry* **1994**, *33*, 3494–3500.
- [39] R. C. Wilmouth, I. J. Clifton, C. V. Robinson, P. L. Roach, R. T. Aplin, N. J. Westwood, J. Hajdu, C. J. Schofield, *Nat. Struct. Biol.* **1997**, *4*, 456–462; P. A. Wright, R. C. Wilmouth, I. J. Clifton, C. J. Schofield, *Eur. J. Biochem.* **2001**, *268*, 2969–2974; E. S. Radisky, J. M. Lee, C.-J. K. Lu, D. E. Koshland, Jr., *Proc. Natl. Acad. Sci. USA* **2006**, *103*, 6835–6840.
- [40] M. W. Larsen, D. F. Zielinska, M. Martinelle, A. Hidalgo, L. J. Jensen, U. T. Bornscheuer, K. Hult, *ChemBioChem* **2010**, *11*, 796–801.
- [41] E. R. Guinto, S. Caccia, T. Rose, K. Fütterer, G. Waksman, E. Di Cera, *Proc. Natl. Acad. Sci. USA* **1999**, *96*, 1852–1857.
- [42] F. Stehle, W. Brandt, C. Milkowski, D. Strack, *FEBS Lett.* **2006**, *580*, 6366–6374.
- [43] Review: C. Milkowski, D. Strack, *Phytochemistry* **2004**, *65*, 517–524.
- [44] P. Bernhardt, K. Hult, R. J. Kazlauskas, *Angew. Chem. Intl. Ed.* **2005**, *44*, 2742–2746; *Angew. Chem.* **2005**, *117*, 2802–2806; D. T. Yin, P. Bernhardt, K. L. Morley, Y. Jiang, J. D. Cheeseman, J. D. Schrag, R. J. Kazlauskas, *Biochemistry* **2010**, *49*, 1931–1942.
- [45] E. J. Corey, K. A. Cimprich, *Tetrahedron Lett.* **1992**, *33*, 4099–4102.
- [46] J. D. Cheeseman, A. Tocilj, S. Park, J. D. Schrag, R. J. Kazlauskas, *Acta Crystallogr. D Biol. Crystallogr.* **2004**, *60*, 1237–1243.
- [47] S. Park, K. L. Morley, G. P. Horsman, M. Holmquist, K. Hult, R. J. Kazlauskas, *Chem. Biol.* **2005**, *12*, 45–52.
- [48] H. J. C. Berendsen, J. P. M. Postma, W. F. van Gunsteren, J. Hermans, *Intermolecular Forces* (Ed.: B. Pullman), Reidel, Dordrecht, **1981**, pp. 331–342.
- [49] G. A. Kaminski, R. A. Friesner, J. Tirado-Rives, W. L. Jorgensen, *J. Phys. Chem. B* **2001**, *105*, 6474–6487.
- [50] H. J. C. Berendsen, J. P. M. Postma, W. F. van Gunsteren, A. Dinola, J. R. Haak, *J. Chem. Phys.* **1984**, *81*, 3684–3690.

Received: November 15, 2010

Published online on February 23, 2011